Anal. Bioanal. Electrochem., Vol. 7, No. 2, 2015, 210-219

Analytical & Bioanalytical Electrochemistry

www.abechem.com

Full Paper

Effect of Accumulative Roll Bonding (ARB) Process on the Electrochemical Behavior of Pure Copper in 0.01 M KOH Solution

Omid Imantalab* and Arash Fattah-alhosseini

Department of Materials Engineering, Bu-Ali Sina University, Hamedan 65178-38695, Iran

* Corresponding Author, Tel.: +98 81 38297400; Fax: +98 81 38257400

E-Mail: o.imantalab@gmail.com

Received: 26 December 2014 / Accepted: 10 April 2015 / Published online: 30 April 2015

Abstract- In this work, effect of accumulative roll bonding (ARB) process on the electrochemical behavior of pure copper in 0.01 M KOH solution were studied. Corrosion current density measured from potentiodynamic polarization plots, the passive film and charge-transfer resistance estimated with electrochemical impedance spectroscopy (EIS) and finally defect density drawn from Mott–Schottky analysis. Potentiodynamic polarization curves revealed that the higher number of cycles for specimens proceeds with the ARB process rather than annealing yield to lower corrosion current density. EIS results showed that as the number of ARB cycles increases, both passive film and the charge-transfer resistance increases. Mott–Schottky analysis revealed that with increasing the number of ARB cycles, the acceptor density of the passive films decreased. All electrochemical measurements showed that increasing the number of ARB cycles offer better conditions for forming the passive films.

Keywords- Accumulative roll bonding, Passive film, Mott–Schottky, Ultra-fine grained copper

1. INTRODUCTION

Severe plastic deformation processes such as high pressure torsion, equal channel angular pressing, and ARB have been used for fabrication high-strength materials with better mechanical behavior. Among these processes, ARB is extensively used for the industrial

production of ultra-fine grained sheets. Indeed, this process is excellent for manufacturing ultra-fine grained plates and sheets [1–5].

Copper are widely used in industrial applications, such as power generation and heat exchanger tubes. In these applications copper have to withstand the alkaline solutions and these solutions can affect the passivation behavior. Therefore, it is important to pay attention to the electrochemical behavior of copper in the alkaline solutions [6–12].

The electrochemical behavior of copper in the alkaline solutions has been studied in correlation to the protective nature of the passive film [13–17]. The characteristics of copper passive film are related to the composition of its. The composition of the passive film formed on copper has been characterized by using different methods. These studies revealed that the composition of the passive film depends on many parameters such as pH, presence of aggressive anions and aerating conditions [18–23].

Although some papers have been published on the mechanical behavior of ultra-fine grained copper and copper alloys [2–5], little study has been focused on the electrochemical behavior of ultra-fine grained copper and copper alloys. Based on the Pourbaix diagram for copper in water (Fig.1), at pH values ranging from 6.8 to 12.8 (passive domain) the surface film formed on copper is protective [24]. In this work, the effect of ARB process on the electrochemical behavior of pure copper in 0.01 M KOH (pH=12) solution was investigated by the potentiodynamic polarization, EIS and Mott–Schottky analysis.

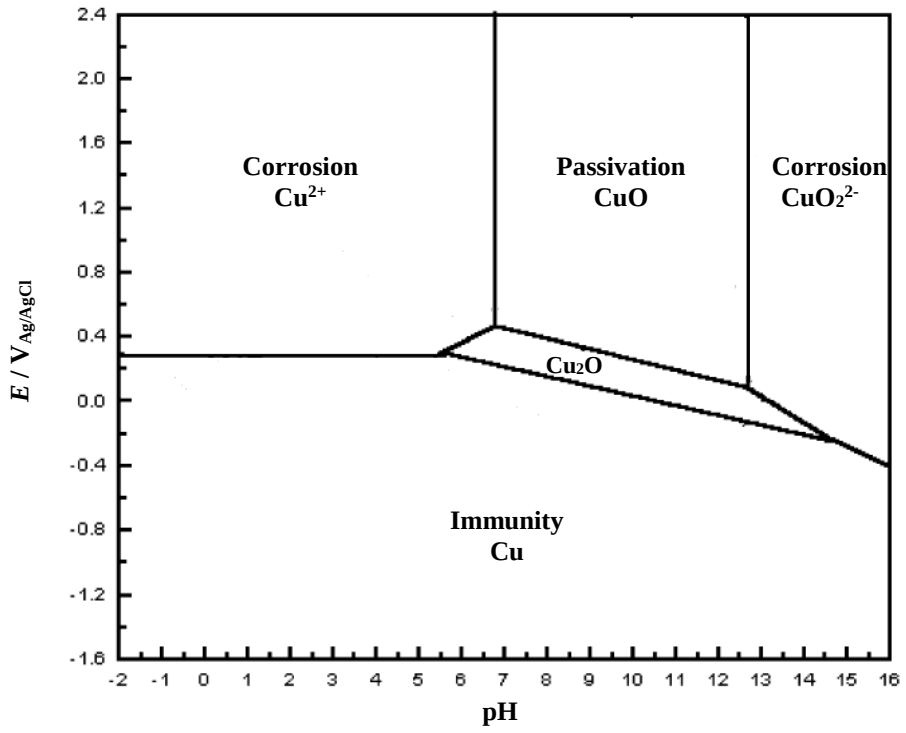

Fig. 1. Pourbaix diagram for copper –water system at 25 °C [24]

2. EXPERIMENTAL PROCEDURES

Before any process, the pure copper (99.96 wt. %) sheets were annealed for 120 min in 480 °C. They were cut in dimensions of 150 mm length, 50 mm width, and 1 mm thickness for the ARB process. To produce a well metallurgical bond by the ARB process, it is essential to remove any contaminations that may be present on the surface of the metals to be joined [1]. Surface preparation was degreased in acetone bath and scratch brushed with stainless steel brush. Generally, the time between surface preparation and rolling was kept down to less than 120 sec. ARB process was carried out with no lubrication, using a laboratory rolling mill with a loading capacity of 20 tons. The roll bonding process was carried out with a specific amount of reduction equal to 50% (equivalent strain of 0.8 per cycle). Then, the roll bonded strips were cut in half. The specimens manufactured up to 2, 4, and 6 cycles were used to evaluate the electrochemical behavior.

All specimens were ground to 2000 grit and cleaned by deionized water prior to tests. All the electrochemical measurements were done in a conventional three-electrode flat cell under aerated conditions by using the μ Autolab Type III/FRA2 system controlled by a personal computer. The counter electrode was a Pt plate, while the reference electrode was Ag/AgCl saturated in KCl. 0.01 M KOH solution was used as the test solutions at 25±1 °C. Prior to electrochemical measurements, working electrodes immersed at open circuit potential (OCP) conditions in solution to form a steady-state passive film. The electrochemical measurements were done in the following sequence:

(a) Potentiodynamic polarization curves were measured potentiodynamically at a scan rate of 1 mV s^{-1} starting from –0.25 V (*vs*. E_{corr}) to 1.0 $V_{Ag/AgCl}$.

(b) EIS test at OCP and AC potential with the amplitude of 10 mV and normally a frequency range of 100 kHz to 10 mHz. For the EIS data modeling and curve-fitting method, the NOVA impedance software was used.

(c) Mott–Schottky analysis was carried out on the passive films at a frequency of 1 kHz using a 10 mV ac signal and a step potential of 25 mV, in the cathodic direction.

3. RESULTS AND DISCUSSION

3.1. Microhardness investigation

Fig. 2 shows the variations in microhardness values of pure copper specimens (Annealed and produced by ARB). The result of microhardness tests showed that by implementing the ARB process the values of microhardness improve with increasing the number of ARB cycles. Also, a drastic increase of microhardness was seen after the two ARB cycle. This increase at low strains can be attributed to the formation of cell wall/subgrain boundaries rather than to grain refinement leading to strain hardening based on the density of dislocations and interactions between them [1,25].

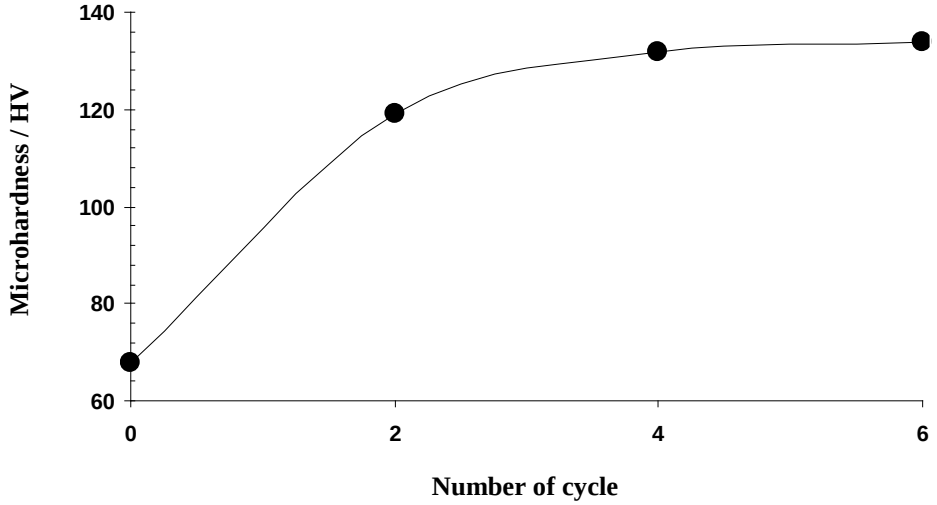

Fig. 2. Microhardness evolution as a function of cycle number for pure copper specimens (annealed sample=zero cycle)

However, by increasing the number of cycles, the rate of microharness improvement decreased. This result clearly show a great grain refinement at the beginning of the process (by implementing the ARB) when the rate of grain refinement by increasing the number of cycles decreased.

3.2. Potentiodynamic polarization measurements

Fig. 3 presents the potentiodynamic polarization curves of pure copper specimens (Annealed and produced by ARB) in 0.01 M KOH solution. All potentiodynamic polarization curves showed that implementing the ARB process led to lower corrosion and passive current densities.

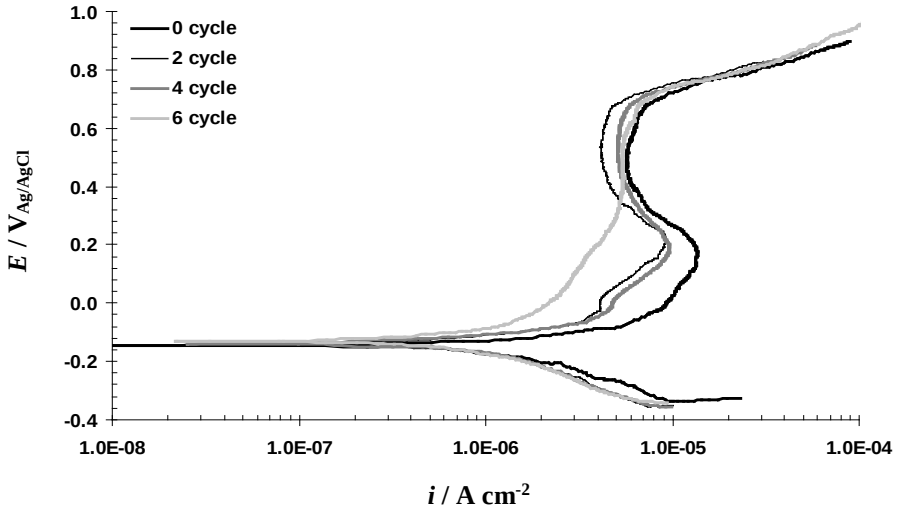

Fig. 3. Potentiodynamic polarization curves of pure copper specimens (Annealed and produced by ARB) in 0.01 M KOH solution (annealed sample=zero cycle)

A remarkable decrease in corrosion and passive current density was observed after 6 ARB cycle. The variation of the corrosion current density (i_{corr}) of pure copper specimens is shown in Fig. 4. The corrosion current density was calculated by Tafel extrapolation of the linear part for the cathodic branch back to the corrosion potential with accuracy of more than 95% [26,27]. It is observed that corrosion current density decreases with increasing number of ARB cycles.

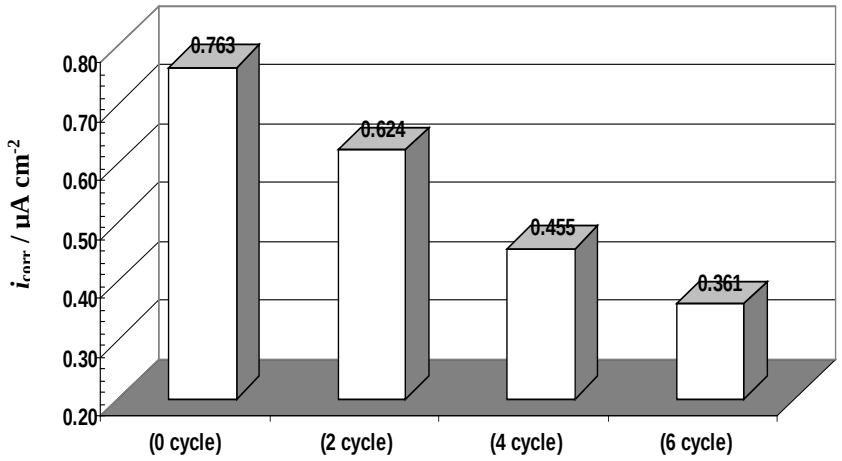

Fig. 4. Corrosion current density evolution as a function of cycle number for pure copper specimens (annealed sample=zero cycle).

3.3. EIS measurements

The EIS response of pure copper specimens (Annealed and produced by ARB) in 0.01 M KOH solution was done at the steady-state corrosion potential and the results are shown as Nyquist plots in Fig. 5. All Nyquist plots show imperfect semicircles.

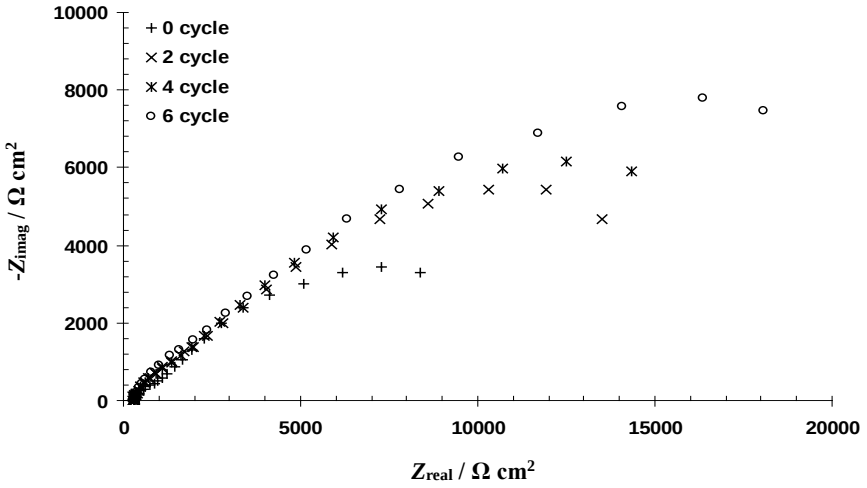

Fig. 5. Effect of number of ARB cycles on the Nyquist plots of pure copper in 0.01 M KOH solution

Also, in Fig. 5 there was an increase of the low frequency impedance with increasing number of ARB cycles. To simulate the measured impedance data, the equivalent circuit shown in Fig. 6 (with two time constants) was used [7]. In this equivalent model, Q_P the constant phase element of the passive film, R_p the passive film resistance, Q_{dl} the constant phase element of the double layer, R_{ct} the charge-transfer resistance, and R_S represents the solution resistance.

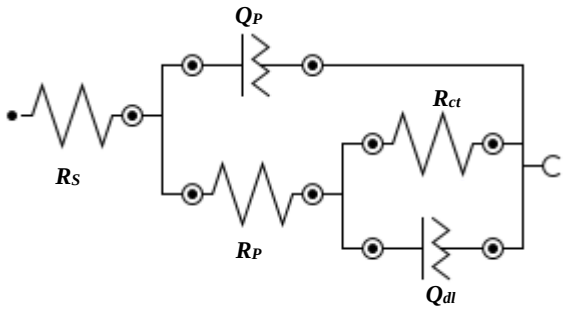

Fig. 6. The best equivalent circuit used to model the experimental EIS data

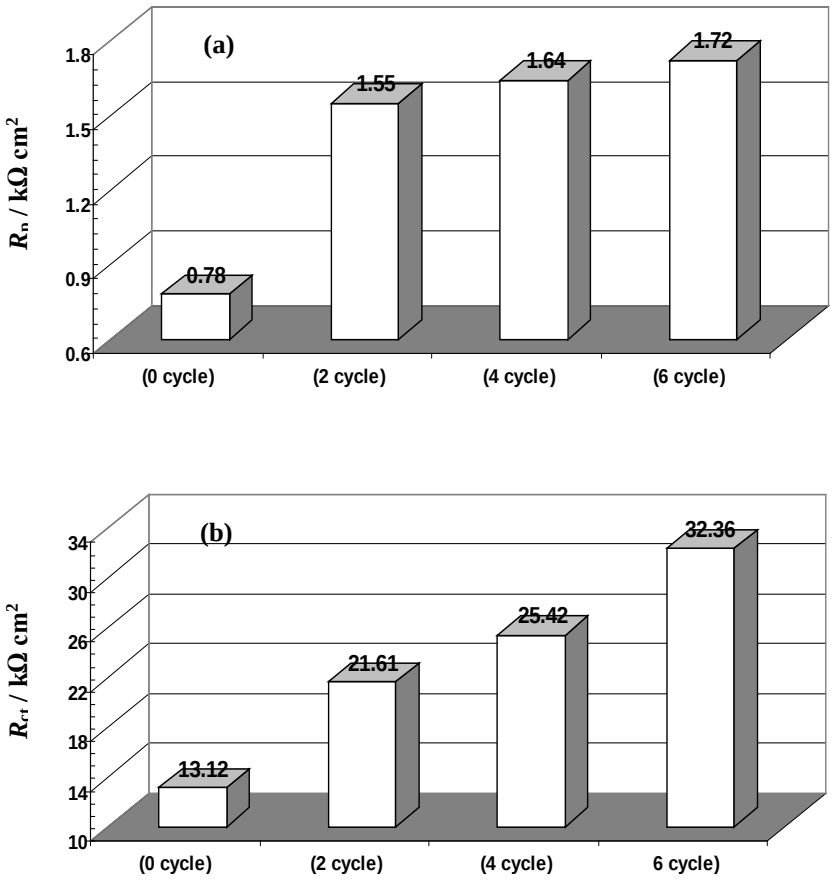

Fig. 7. Effect of number of ARB cycles on the (a) passive film resistance (R_p) and (b) charge-transfer resistance (R_{ct}) of the passive films formed on pure copper in 0.01 M KOH solution

The variation of the passive film resistance (R_p) and the charge-transfer resistance (R_{ct}) of the passive films formed on pure copper specimens (Annealed and produced by ARB) in 0.01 M KOH solution are illustrated in Fig. 7. It is observed that as the number of ARB cycles increases, both passive film and the charge-transfer resistance increases. Therefore, the measured value of polarization resistance ($=R_p+R_{ct}$) increases with increasing the number of ARB cycles, indicating that the corrosion current density decreases with increase the number of ARB cycles.

It is clear that increasing number of ARB cycles give better conditions for forming the passive films with higher protection behavior. Indeed, the ARB process caused to acquiring ultra-fine grained copper with a large fraction of grain boundaries and high internal energy. Moreover, on the side of grain boundaries and inside some grains, the dislocation density and residual stress are high. In this manner, high residual stress prepares the ultra-fine grained copper more nuclei to form denser passive film, improving the corrosion resistance. Also, the formation of ultra-fine grained structures provides the passive film grow more rapidly [28].

3.4. Mott-Schottky analysis

Fig. 8 shows the Mott-Schottky plots of pure copper specimens (Annealed and produced by ARB) in 0.01 M KOH solution where by increasing the number of ARB cycles, capacitances clearly increase.

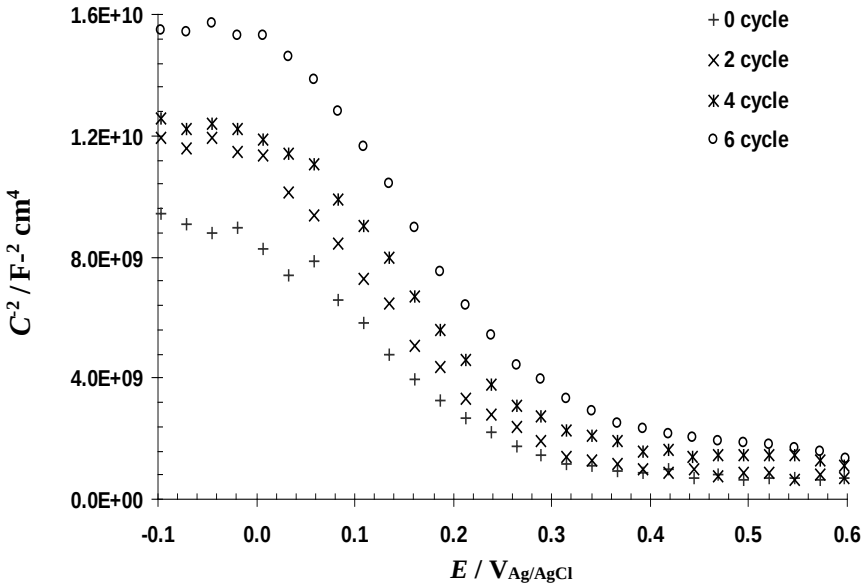

Fig. 8. Mott-Schottky plots of pure copper specimens (Annealed and produced by ARB) in 0.01 M KOH solution

Also, in all plots there is a region in which C^{-2} and E possess a somehow linear relationship. The negative slope in this region is attributed to p-type behavior and according to Eq. (1), acceptor density has been determined from these positive slopes [14–17]:

$$\frac{1}{C^2} = -\frac{2}{\varepsilon\varepsilon_0 e N_A}\left(E - E_{FB} - \frac{kT}{e}\right) \quad (1)$$

where e is the electron charge, N_A represents the acceptor density for p-type semiconductors (cm^{-3}), ε stands for the dielectric constant of the passive film, ε_0 denotes the vacuum permittivity, *k, T, and* E_{FB} are the Boltzmann constant, absolute temperature, and flat band potential, respectively. The flat band potential can be determined from the extrapolation of the linear portion to $C^{-2}=0$ [30]. $\frac{k_B T}{q}$ can be negligible as it is only about 25 mV at room temperature [30]. For calculation of N_A, a value of dielectric constant $\varepsilon=12$, which was estimated by Wu et al [29], was used for the passive films on copper and its alloys.

Fig. 9 shows the calculated acceptor density of pure copper specimens (Annealed and produced by ARB) in 0.01 M KOH solution. According to Fig. 9, the acceptor density decreases with the number of ARB cycles. Point defect model has been used to provide an excellent description of the passive film growth. Using this model we obtained quantitative analysis of the passive film as well as an analytical expression for the flux and concentration of vacancies within the passive film [26]. Based on the point defect model, the cation vacancies are electron acceptors, thereby doping the barrier layer p-type, whereas the oxygen vacancies and the metal interstitials are electron donors, resulting in the n-type doping [22]. The orders of magnitude of the acceptor density are around 10^{20} cm^{-3} and are comparable to those reported in other studies [30]. These high values of the acceptor density can be attributed to a higher density of the Cu vacancies in the passive films.

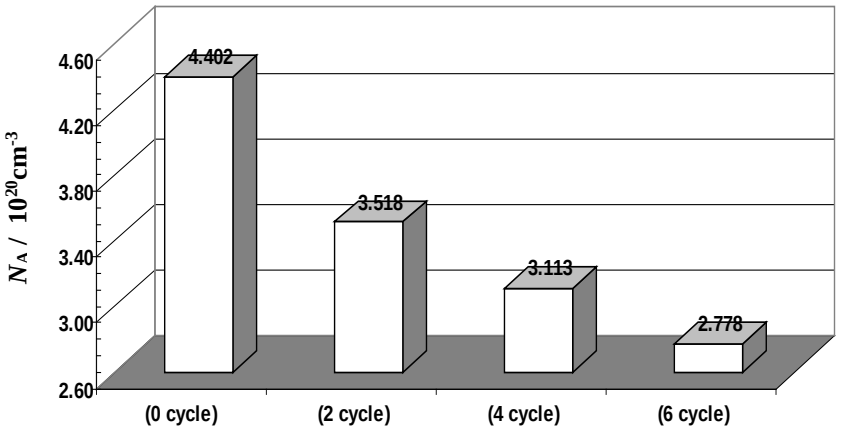

Fig. 9. Calculated acceptor density of the passive films formed on pure copper in 0.01 M KOH solution

4. CONCLUSIONS

Effect of ARB process on the electrochemical behavior of pure copper in 0.01 M KOH solution (pH=12) was investigated. Conclusions drawn from the study are as follows

1. The microhardness tests showed that by implementing the ARB process the values of microhardness improve with increasing the number of ARB cycles.
2. These plots showed that the higher number of cycles for specimens proceed with the ARB process rather than annealing yield to lower corrosion and passive current densities.
3. EIS results showed that as the number of ARB cycles increases, both passive film and the charge-transfer resistance increases.
4. Mott–Schottky analysis revealed that with increasing the number of ARB cycles, the acceptor density of the passive films decreased.

REFERENCES

[1] M. R. Rezaei, M. R. Toroghinejad, and F. Ashrafizadeh, J. Mater. Process. Tech, 211 (2011) 1184.
[2] S. Pasebani, and M. R. Toroghinejad, Mater. Sci. Eng. A 527 (2010) 491.
[3] S. Pasebani, M. R. Toroghinejad, and M. Hosseini, J. Szpunar, Mater. Sci. Eng. A 527 (2010) 2050.
[4] F. Salimyanfard, M. R. Toroghinejad, F. Ashrafizadeh, M. Hoseini, and J. A. Szpunar, Mater. Des. 44 (2013) 374.
[5] H. Miyamoto, K. Harada, T. Mimaki, A. Vinogradov, and S. Hashimoto, Corros. Sci. 50 (2008) 1215.
[6] P. Shi, Q. Wang, Y. Xu, and W. Luo, Mater. Lett. 65 (2011) 857.
[7] J. J. Shim, and J. G. Kim, Mater. Lett. 58 (2004) 2002.
[8] Q. Zhong, L. Yu, Y. Xiao, Y. Wang, Q. Zhou, and Q. Zhong, Advanc. Mater. Res. 785 (2013) 928.
[9] M. M. Antonijevic, S. C. Alagic, M. B. Petrovic, M. B. Radovanovic, and A. T. Stamenkovic, Int. J. Electrochem. Sci. 4 (2009) 516.
[10] A. M. Alfantazi, T. M. Ahmed, and D. Tromans, Mater. Des. 30 (2009) 2425.
[11] J. Kunze, V. Maurice, L. H. Klein, H. H. Strehblow, and P. Marcus, Corros. Sci. 46 (2004) 245.
[12] G. Kear, B. D. Barker, and F. C. Walsh, Corros. Sci. 46 (2004) 109.
[13] D. W. Shoesmith, T. E. Rummery, D. Owen, and W. Lee, J. Electrochem. Soc. 123 (1976) 790.
[14] Y. Ashworth, and D. Fairhurst, J. Electrochem. Soc. 124 (1977) 506.
[15] R. M. Souto, S. Gonzalez, R. C. Salvarezza, and A. J. Arvia, Electrochim. Acta 39 (1994) 2619.

[16] M. Pérez Sánchez, M. Barrera, S. González, R. M. Souto, R. C. Salvarezza, and A. J. Arvia, Electrochim. Acta 35 (1990) 1337.
[17] M. M. Laz, R. M. Souto, S. González, R. C. Salvarezza, and A. J. Arvia, Electrochim. Acta 37 (1992) 655.
[18] D. W. Soesmith, T. E. Rummery, D. Owen, and W. Lee, J. Electrochem. Soc. 123 (1976) 790.
[19] W. Kautek, M. Geub, M. Sahre, P. Zhao, and S. Mirwald, Surf. Interface Anal. 25 (1997) 548.
[20] W. Kautek, and J. G. Gordon, J. Electrochem. Soc. 137 (1990) 2672.
[21] H. D. Speckmann, S. Haupt, and H. H. Streblow, Surf. Interface Anal. 11 (1988) 148.
[22] Y. Ling, M. Taylor, S. Sharifiasl, and D. D. Macdonald, ECS Transactions 50 (2013) 53.
[23] W. A. Badawy, and F. M. AI-Kharafi, Corros. 55 (1999) 268.
[24] M. Pourbaix, Atlas of Electrochemical Equilibria in Aqueous Solutions, 2nd ed., NACE, Houston, (1974).
[25] M. Shaarbaf, and M. R. Toroghinejad, Mater. Sci. Eng. A 473 (2008) 28.
[26] S. O. Gashti, and A. Fattah-alhosseini, Anal. Bioanal. Electrochem. 6 (2014) 535.
[27] A. Fattah-alhosseini, and M. Sabaghi Joni, J. Magnesium Alloy. 2 (2014) 175.
[28] M. F. Naeini, M. H. Shariat, and M. Eizadjou, J. Alloys Comp. 509 (2011) 4696.
[29] H. Wu, Y. Wang, Q. Zhong, M. Sheng, H. Du, and Z. Li, J. Electroanal. Chem. 663 (2011) 59.
[30] K. Nakaoka, J. Ueyama, and K. Ogura, J. Electrochem. Soc. 151 (2004) C66.